Importance of melting in the mantle

1. Information on upper mantle temperature
   - mid-ocean ridges
   - hotspots
2. Lens through which we view chemistry and isotopic composition of the mantle
3. Information on mantle dynamics
4. Models for chemical differentiation of the Earth

Outline

1. Properties of silicate liquids
2. Adiabatic decompression melting
   - Melting temperature(s) of lherzolite
   - Model for mid-ocean ridges
3. Melting in mantle plumes
4. Effects of water and pyroxenite/eclogite veins
5. Phase equilibria of melting (only the basics)
6. Melt percolation models..... U series isotopes

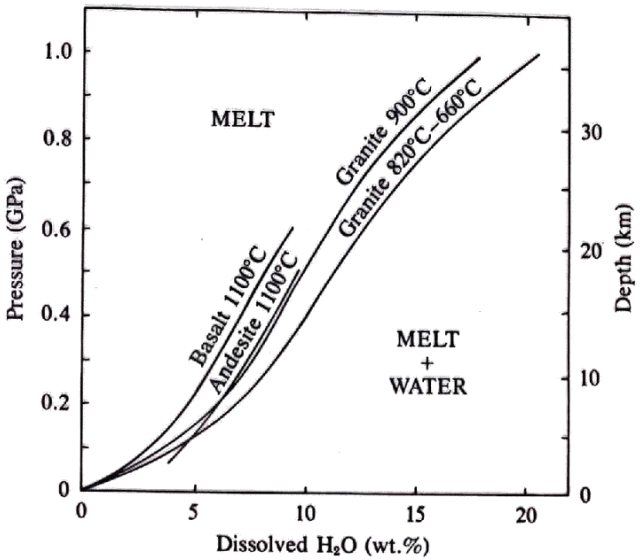

Figure 7-4 Solubility of water in selected silicate melts. To the right of a particular curve at the specified T, the system contains more water than can be dissolved in the melt and the system consists of hydrous melt plus a separate water phase whose density depends upon P (see Figure 7-2). To the left of a curve, the solubility limit is not exceeded and all of the water is dissolved in the melt. [After I. S. E. Carmichael, F. J. Turner, and J. Verhoogen, 1974, *Igneous Petrology* (New York: McGraw Hill).]

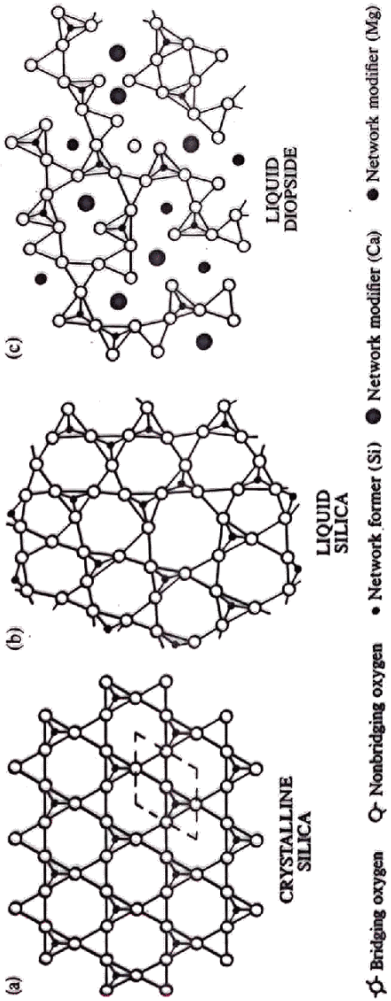

Figure 7-5 Conceptual models of atomic structures of silicate melts (see Carmichael and others, 1974, p. 133) with a model of a crystalline solid for comparison. (a) Crystalline silica (high tridymite). Layers of hexagonal rings of Si–O tetrahedra with alternating apices pointing up and down are stacked on top of one another, creating a three-dimensional structure in which each oxygen is shared by two silicons. Tetrahedra with apices pointing up have the upper apical oxygen left out of drawing so as to reveal underlying silicon. Dashed line indicates outline of one unit cell. (b) Model of liquid silica. Si–O tetrahedra are only very slightly distorted. Long-range order is absent. Structure is very highly polymerized, with all tetrahedra interconnected. (c) In this model of liquid diopside, there is less polymerization than in liquid silica. Note presence of network modifiers.

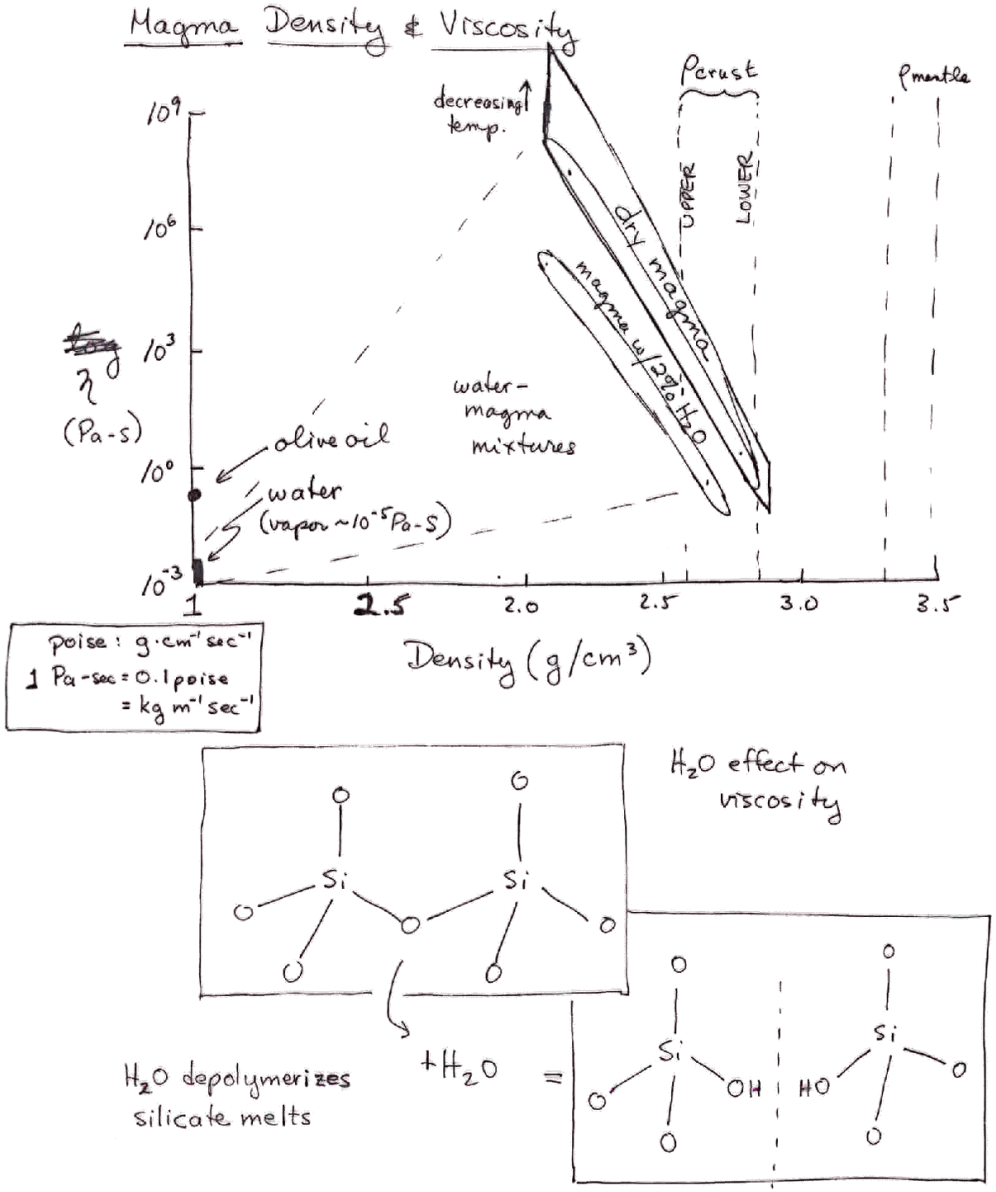

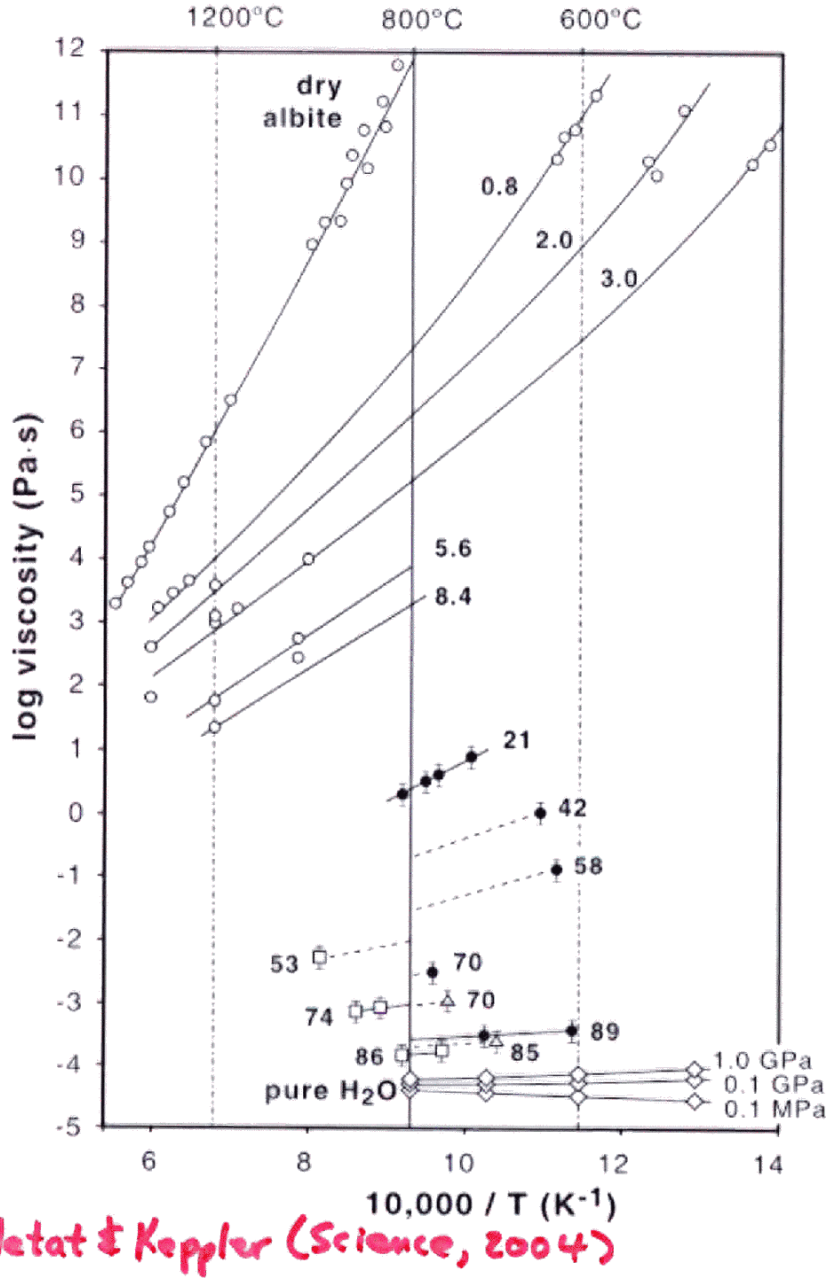

Audetat & Keppler (Science, 2004)

Fig. 2. Arrhenius plot showing the viscosity of fluid-melt solutions in the entire range from pure silicate melt to pure H_2O. Diamonds and open circles correspond to literature values of pure H_2O (*13*) and albite melts with <10 wt % H_2O (*27*), respectively. Our measurements are represented by filled circles (albite-H_2O), open squares (leucite-H_2O), and open triangles (pectolite-H_2O). Bold numbers refer to water contents in wt % H_2O. Also shown are extrapolations of the measured viscosities to a fixed temperature of 800°C (vertical solid line), which allowed the construction of Fig. 3.

Appendix B

Calculation of Densities and Viscosities of Silicate Melts

Density

The calculation given below is based on the method of Bottinga and Weill (1970, Amer. J. Sci., 269: 169-182) but uses more recently determined values of molar volumes. The original analysis, in weight percent, is recalculated to molecular proportions water-free in the manner explained in Appendix A but without renormalizing to 100 percent.
T = (temperature in °C - 1400) x 10^{-5}

Z1 = SiO_2 x 27.03
Z2 = TiO_2 x 22.6 x (1 + T x 26.7)
Z3 = $AlO_{1.5}$ x 36.63/2 x (1 + T x 14.7)
Z4 = $FeO_{1.5}$ x 43.73/2 x (1 + T x 12.2)
Z5 = (FeO + MnO) x 13.85 x (1 + T x 31.2)
Z6 = MgO x 11.43 x (1 + T x 9.4)
Z7 = CaO x 16.32 x (1 + T x 38.4)
Z8 = $NaO_{0.5}$ x 14.39 x (1 + T x 23.5)
Z9 = $KO_{0.5}$ x 22.965 x (1 + T x 24.9)

Density = 100 / (Z1 + Z2 + Z3 + Z4 + Z5 + Z6 + Z7 + Z8 + Z9)

Viscosity

The calculation below is based on the method of H. R. Shaw (1972, Amer. J. Sci., 272: 870-893). It gives the viscosity, η, of crystal-free silicate melts in poise in log units. Weight percentages of the oxide components are first recalculated to 100 percent then converted to cation proportions, as shown below. Temperature (T) is in degrees K.

SI = SiO_2 / 60.0843
TI = TiO_2 / 79.8988
Al = Al_2O_3 / 50.9806
F3 = Fe_2O_3 / 79.8461
F2 = FeO / 71.8461
MN = MnO / 70.9374
Mg = MgO / 40.3044
CA = CaO / 56.9895
Na = Na_2O / 30.9895
K = K_2O / 47.0980
H = H_2O / 18.0152
P = P_2O_5 / 70.9723
Normalize to 100
FM = F3 + F2 + MN + MG
NK = N + K
C = SI + TI + AL + FM + CA + (NK + P)/2 + H
Q1 = AL x 6.7
Q2 = FM x 3.4
Q3 = (CA + TI) x 4.5
Q4 = NK x 1.4
Q5 = H x 2
QT = (Q1 + Q2 + Q3 + Q4 + Q5) x $SI/C^{\frac{2}{3}}$
X = (QT/(1- SI/C) x (10000/T - 1.5) - 6.4
Log η = X/2.303, $\eta = e^X$

MK Parent magma	
Oxide	wt %
SiO2	48.0
TiO2	2.1
Al2O3	10.8
Fe2O3	2.0
FeO	10.0
MnO	0.2
MgO	15.0
CaO	8.8
Na2O	2.0
K2O	0.3
H2O	0.0
P2O5	0.2
	99.34

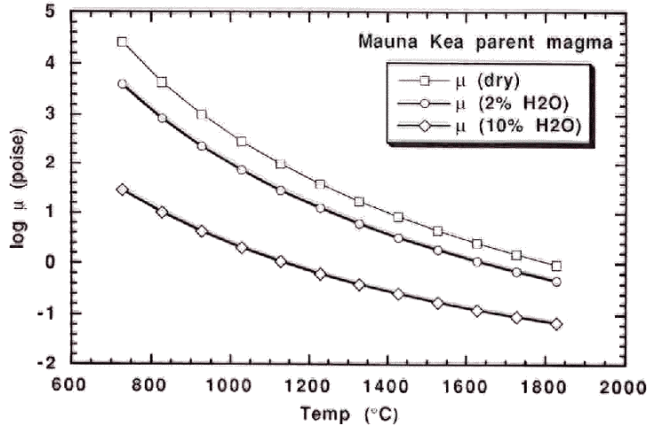

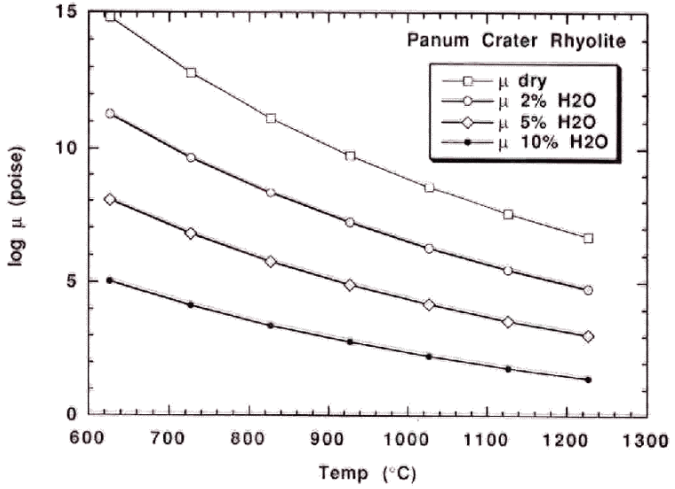

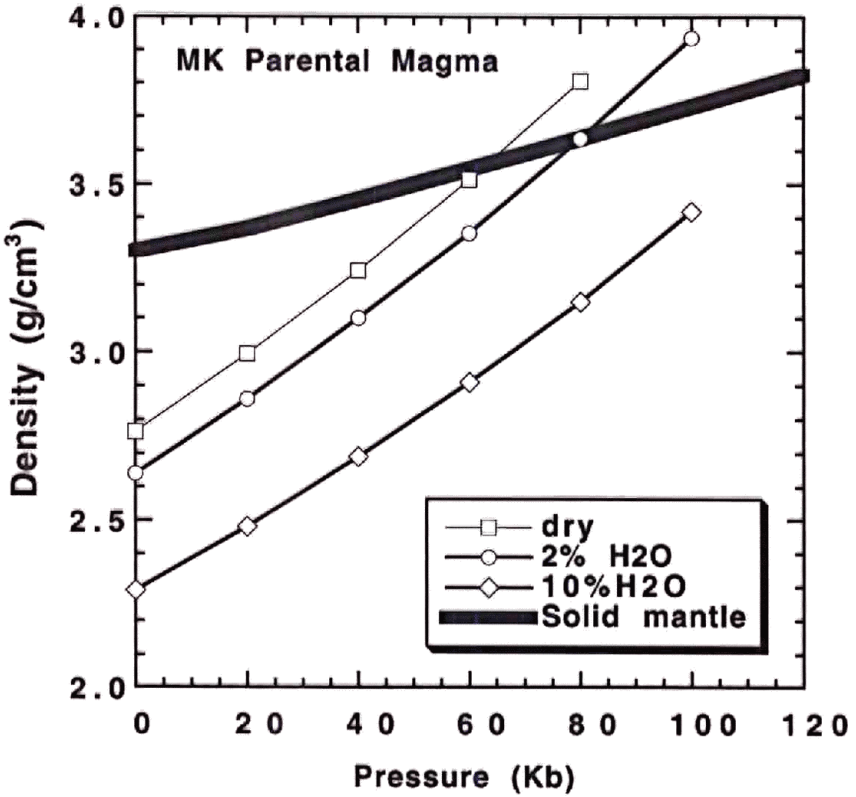

STOLPER ET AL.: MELT SEGREGATION, PARTIALLY MOLTEN SOURCE REGIONS

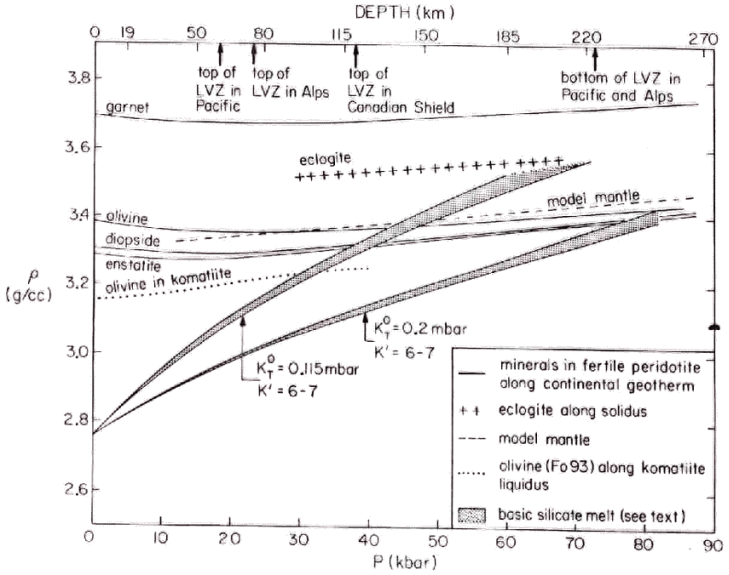

Fig. 2. Comparison of the density of basic silicate melt, calculated using (1) and the parameters discussed in the text, and the densities of possible mantle rocks and minerals. The model mantle is from *Dziewonski et al.* [1975]. The density of eclogite at its solidus is after *Clark and Ringwood* [1964], corrected to the eclogite solidus of *Howells et al.* [1975] using a volume coefficient of thermal expansion of $2 \cdot (10^{-5})$ °C^{-1}. High pressure densities of individual minerals in 'fertile' garnet lherzolite were calculated along the continental geotherm [*Mercier and Carter*, 1975] from (1) using the measured 1 atm densities given by *Boyd and McCallister* [1976], volume coefficient of thermal expansion data from *Skinner* [1966] and *Cameron et al.* [1973] and bulk moduli and their *P–T* derivatives from *Levien et al.* [1979], *Soga* [1967], *Graham and Barsch* [1969], *Liebermann and Mayson* [1976], and *Olinger* [1977]. Densities of olivine (Fo 93) along a komatiite liquidus [*Bickle et al.*, 1977] were calculated in the same way, using a 1 atm density based on *Hazen* [1977] and the bulk modulus from sources cited above. Approximate depths to top and bottom of low-velocity zone are from *Dorman* [1969].

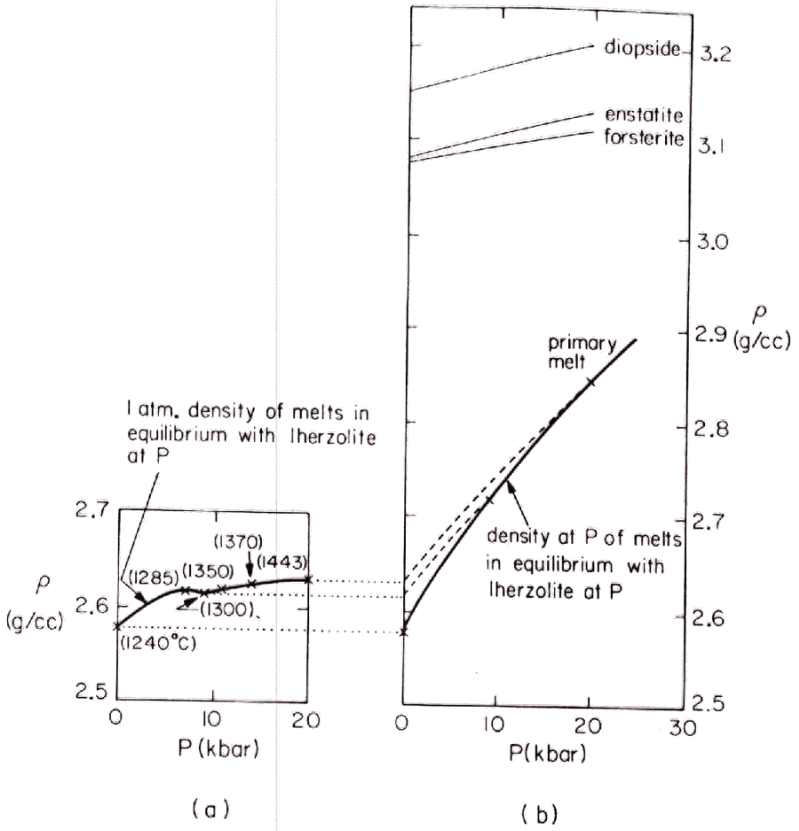

Fig. 3. (*a*) One atmosphere densities of liquids in equilibrium (at pressures between 1 atm and 20 kbar) with olivine + enstatite + diopsidic clinopyroxene + (anorthite ± spinel) in the system CaO–MgO–Al_2O_3–SiO_2 at the temperatures of their equilibration with the lherzolite assemblage [*Presnall et al.*, 1979] calculated from *Bottinga and Weill* [1970]. (*b*) Densities of liquids shown in Figure 3*a* calculated at the pressures of their equilibration with a lherzolitic assemblage using (1) and the parameters given in the text. Also shown are the calculated densities of the forsterite, enstatite, and diopside in the lherzolitic assemblages, calculated as described for Figure 2, using 1 atm densities for the Mg and member minerals

Formation of Magma in the Earth

- Magma is produced mainly in the mantle (generally temp. is not high enough in the crust)
- The magma produced by melting the mantle is basalt (~45 to 50% SiO_2)
- When the mantle rock melts, it melts only partially (up to 10% or 20%)
- The molten material (magma) is less dense than the solid
  - magma $\rho \approx 2.9 g/cm^3$ (or 2900 kg/m^3)
  - solid (olivine + pyroxenes) $\rho \approx 3.4 g/cm^3$ (3400 kg/m^3)
- Magma tends to flow upward, around the solid grains & through channels, in the partially molten mantle
- Magma collects beneath the lithosphere & then gets to the surface mainly through dikes

- Magma forms in the mantle by two processes
  - adiabatic decompression
  - volatile fluxing
- Adiabatic decompression occurs where the mantle rock material is flowing upward as a consequence of mantle convection
  - mid-ocean ridges (MOR)
  - hot spots or mantle plumes
- Volatile fluxing occurs in subduction zones and is responsible for producing island arc volcanoes

To understand adiabatic decompression melting we need to consider the pressure-temperature phase diagram of mantle peridotite

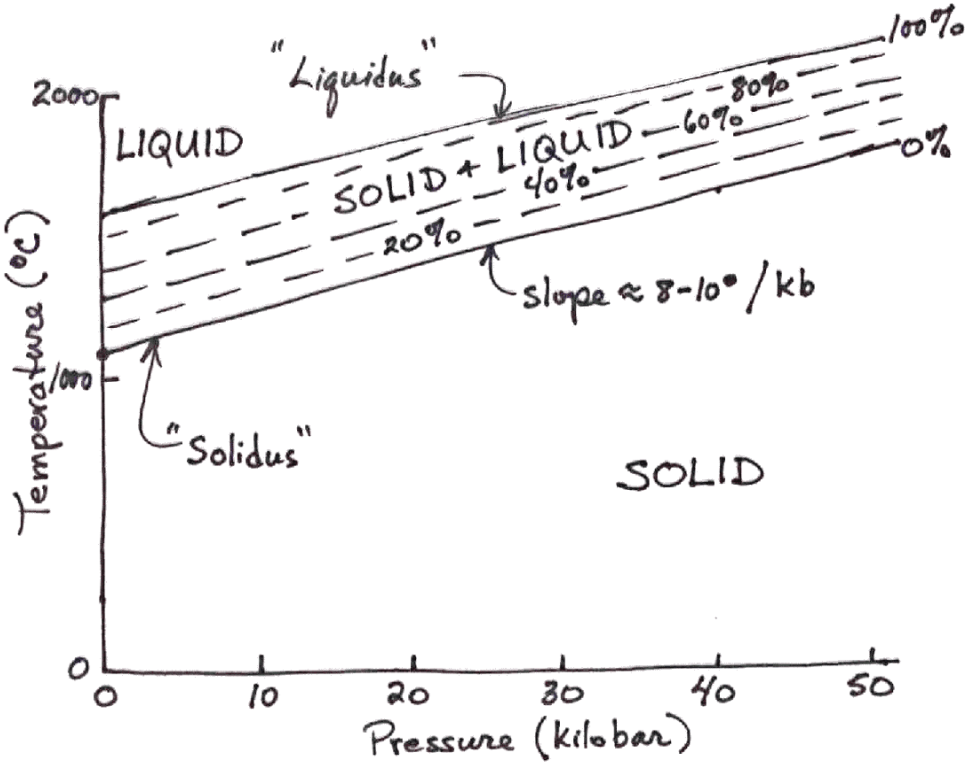

Mantle rock = "Lherzolite"

Olivine + Orthopyroxene + Clinopyroxene

50+% ~20% ~10%

+ Garnet or Spinel

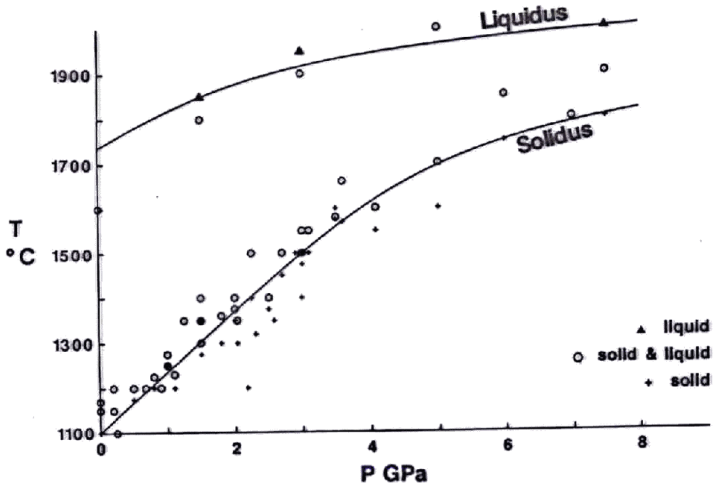

FIG. 5. Experimental determinations of the solidus and liquidus of garnet peridotite. The curves were determined by minimizing $|T_{obs} - T_{calc}|$ and are generated from equations (18) and (19). The data points for the solidus are from Ito & Kennedy (1967), (0, —, 1150), (2.04, 1300, 1350), (2·18, 1200, —), (2·31, 1320, —), (2·58, 1350, —), (2·99, 1400, 1500), (4·08, 1550, 1600), Green & Ringwood (1967*b*), (1·8, 1300, 1360), (2·25, 1400, 1500), (2·7, 1450, 1500), (2·9, 1500, —), (3·1, 1500, 1550), (3·6, 1570, 1660) Jaques & Green (1980), (0, —, 1170), (0·25, —, 1100), (0·2, —, 1150), (0·5, —, 1200), (0·675, —, 1200), (0·9, —, 1200), (1, —, 1250), (1·5, —, 1350), (0·2, —, 1200), (0·5, —, 1200), (1, —, 1250), (1·5, —, 1350), Stolper (1980), (1, —, 1250), (1·5, —, 1350), (2, —, 1400), Harrison (1981), (3·5, 1575, 1580), Takahashi & Kushiro (1983), (0, 1100, 1150), (0·5, 1175, 1200), (0·8, 1200, 1225), (1·1, 1200, 1230), (1·5, 1275, 1300), (2·, 1350, 1375), (2·5, 1375, 1400), (3, 1475, 1500), and Takahashi (1986), (0, 1100, 1150), (0·5, 1175, 1200), (1, 1250, 1275), (1·25, —, 1350), (1·5, 1350, 1400), (2, 1350, 1400), (3, 1500, 1550), (3·5, 1600, —), (5, 1600, 1700), (6, 1750, 1850), (7, —, 1800), (7·5, 1800, 1900). The first entry inside the brackets is the pressure in GPa, the second the highest temperature in °C at which no melt was present, and the third the lowest temperature at which melt was present. If either the second or the third entry is marked with —, the appropriate temperature bound cannot be determined from the experiment. The data points for the liquidus are from Takahashi (1986) (0, 1600, —), (1·5, 1800, 1850), (3, 1900, 1950), (5, 2000, —), (7·5, 1900, 2000), where the second entry is the highest temperature at which solid was still present, and the third entry the lowest temperature at which there was no solid.

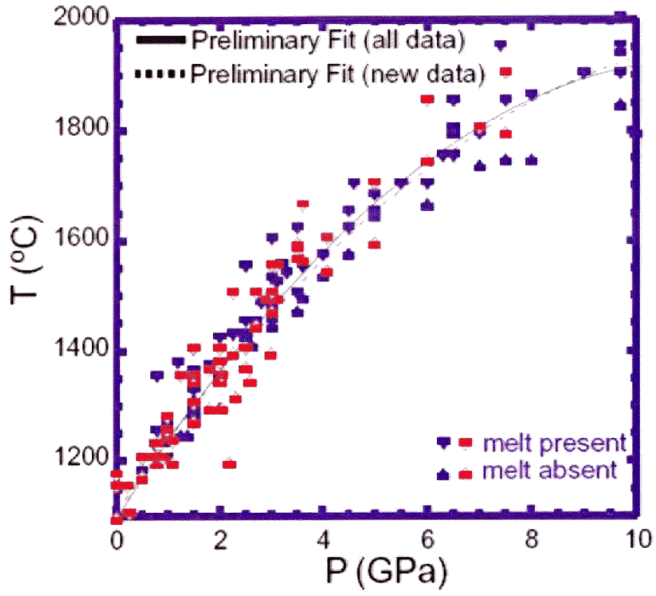

Figure 1. Experimental constraints on the solidus of natural peridotite. Arrows pointing down are experiments in which melt was detected; those pointing up are subsolidus experiments. Solid symbols are from the post-1988 compilation in this paper (references in Table 1); open symbols are from the pre-1988 compilation of *McKenzie and Bickle* [1988]. Best fits to these data, discussed in the text, include the best fit to all the data (solid curve), the best fit to the post-1988 data (dashed line).

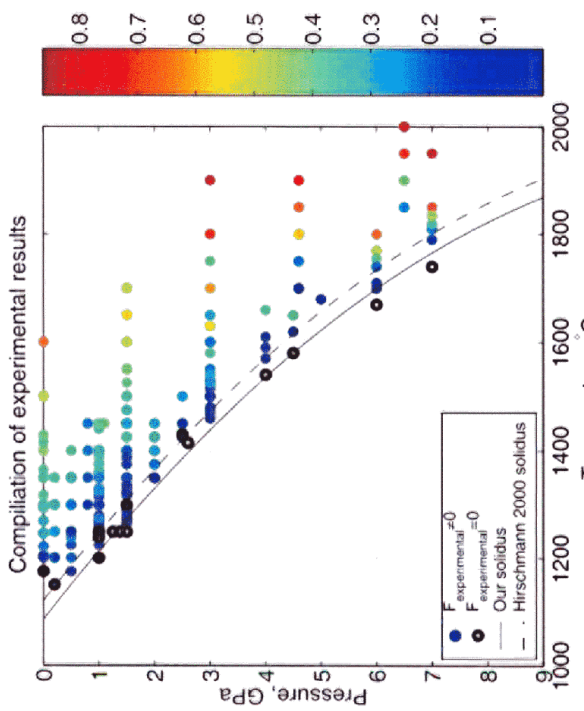

Figure 7. A plot of experimentally determined degree of melting as a function of pressure and temperature. The chosen solidus has an A_1 35°C below that of *Hirschmann* [2000] to better fit the low melt fraction experiments but uses the same A_2 and A_3 that he reported. The 29 experiments within 10°C of the Hirschmann solidus have an average degree of melting of 10 wt%. Of the 29, only 5 have no melting. This is due in part to our inclusion of experiments with more fertile source compositions (e.g., PHN-1611 and MPY) in the database.

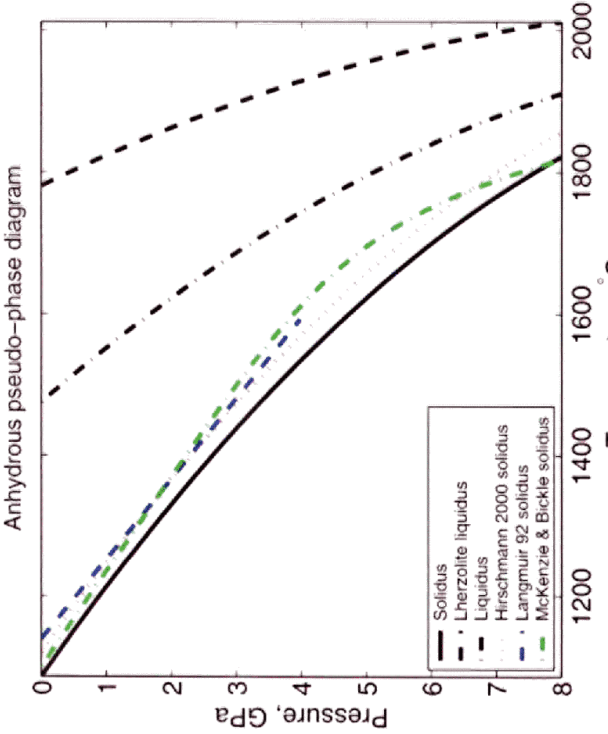

Figure 1. The anhydrous solidus, lherzolite liquidus (see text) and liquidus. Also shown, for comparison, the anhydrous solidi of *Hirschmann* [2000], *Langmuir et al.* [1992], and *McKenzie and Bickle* [1988].

Making magma in the mantle

1. Pressure and depth in the upper mantle and crust.

$$\frac{dP}{dz} = \int_0^z \rho(z) g\, dz$$

for crust $\rho \approx 2.8\ g/cm^3$

for mantle $\rho \approx 3.3\text{-}3.4\ g/cm^3$ (2800 or 3300 kg/m^3)

for crust:

$$P \approx \rho_{crust}\, g\, z \qquad P(kb) \approx .28\, z\,(km)$$

or $z \approx 3.5\, P$

for mantle:

$$P = (\rho_{crust}\, g\, \Delta z_{crust}) + \rho_{mantle}\, g\, (z - \Delta z_{crust}) \quad \underline{\text{continents}}$$

$$P = (\rho_{H_2O}\, g\, \Delta z_{ocean}) + \rho_{crust}\, g\, \Delta z_{crust} + \rho_{mantle}\, g\, (z - z_{crust}) \quad \underline{\text{oceans}}$$

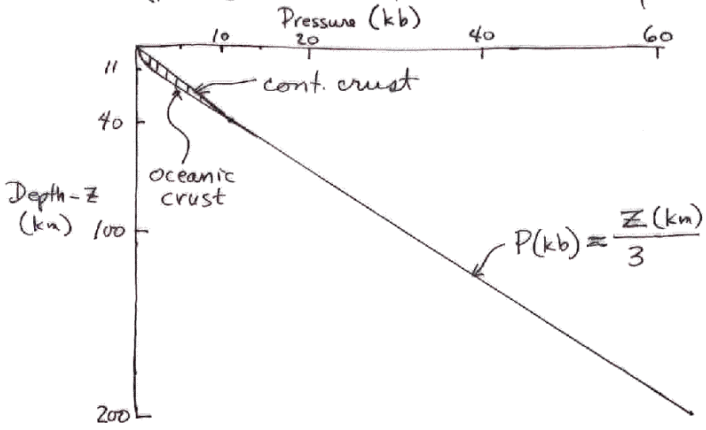

2. Adiabatic movement of mantle rock

(adiabatic = without loss ~~of~~ gain of heat)

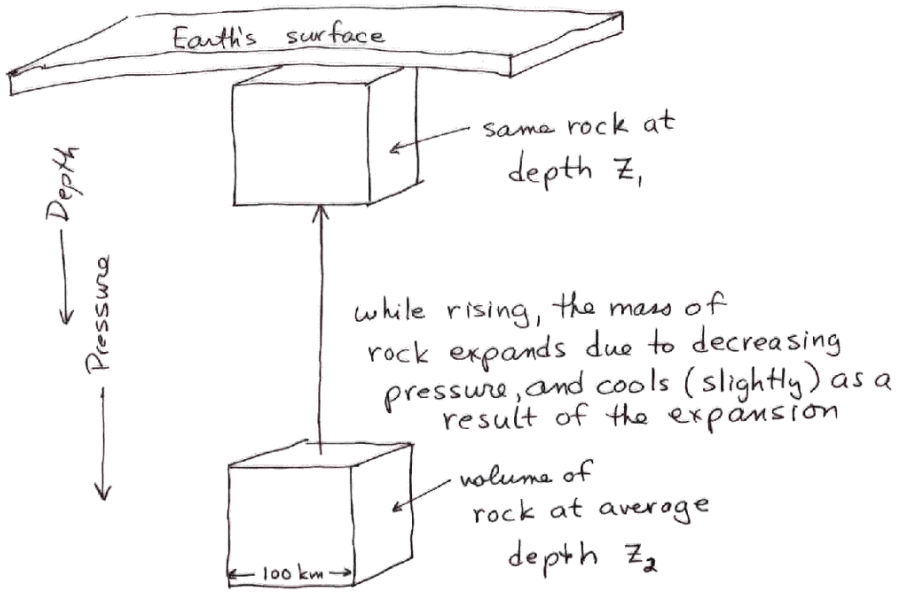

From thermodynamics, it is possible to calculate the change in temperature with pressure:

$$\left(\frac{dT}{dP}\right)_{adiabatic} = \frac{T\alpha}{\rho_{mantle}\, C_p} \qquad \text{or} \qquad \frac{d\ln T}{dP} = \frac{\alpha}{\rho C_p}$$

For typical values, $\frac{dT}{dP} \approx 1°C/kb$ or $0.33°C/km$

3. Why adiabatic?

- Time it takes to rise (or sink) 100km ≈ 10^6 years
  (10^7cm at 10cm/yr)

- Time it takes to cool a cube of rock 100km wide

$$\tau_{cool} \approx \frac{X^2}{\chi} = \frac{(5\times10^6\,cm)^2}{(0.01\,cm^2/sec)} = 25\times10^{14}\,sec$$

$$\equiv 80\times10^6\,years$$

— So the "adiabatic assumption" is good, as long as the width of the upflowing mantle is ~100km or more.

— Slabs going down into the mantle are not adiabatic. The subducting oceanic crust is cold and only ~10km thick; so $\tau_{cool} \approx \tau_{sink}$

The main point is that mantle flowing upward toward the Earth's surface cools slowly. It can move upward 100km and cool by only 33°C.

By contrast, the melting temperature of the mantle (mantle "solidus" temperature) can change by 300°C to 400°C over 100km of depth

④

4. The "potential temperature"

- the potential temperature of the mantle at any depth, z, is the temperature that it would have if it were brought to the surface adiabatically.

- potential temperature is written as either T_p or Θ (theta).

$$T_p = T(z)\, e^{-(\alpha g z / C_p)}$$

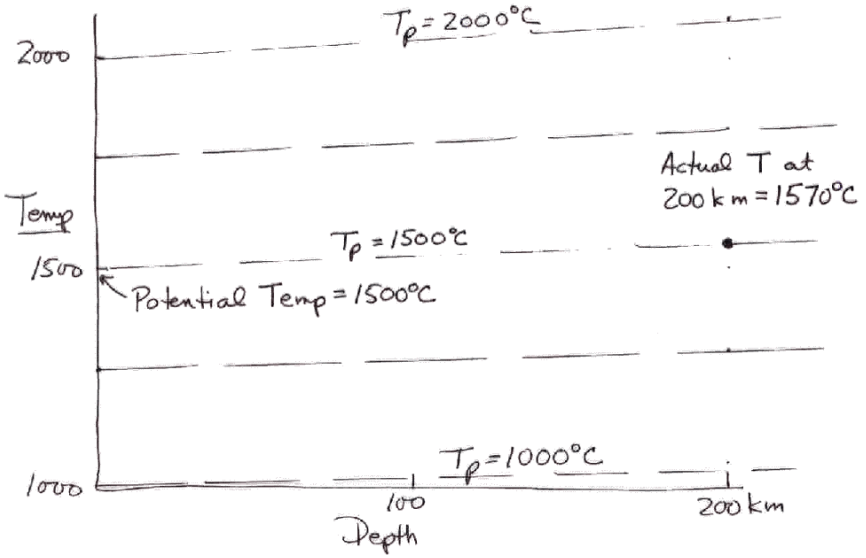

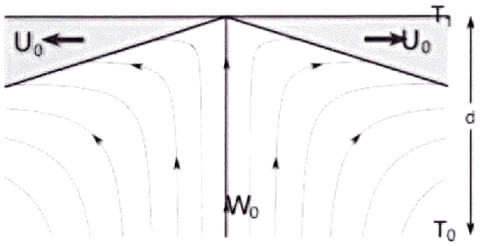

a

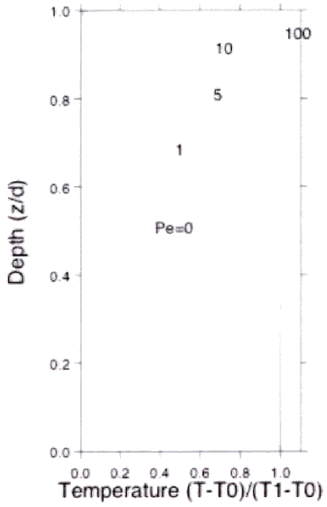

b

$$\mathrm{Pe} = \frac{W_0 d}{\kappa}$$

Pe ≈ 100 for
W_0 = 3 cm/yr

642 D. McKENZIE AND M. J. BICKLE

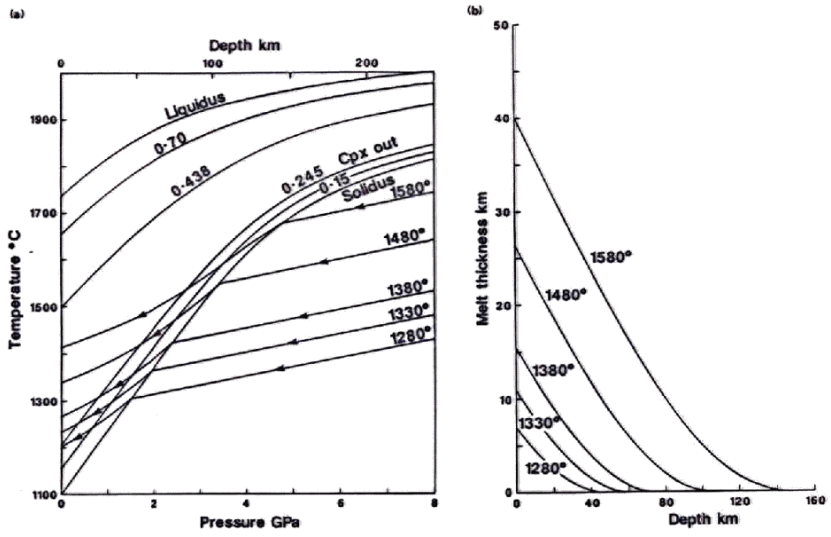

FIG. 7. (a) Adiabatic decompression paths calculated using the equations given by McKenzie (1984*a*) Appendix D, a fourth order Runge–Kutta scheme and

$$\Delta S = 250\ \mathrm{J\,kg^{-1}\,°C^{-1}}.$$

The curves are labelled with their potential temperatures, and entropy is conserved to 1 part in 10^4 during the numerical integration. The curves between the solidus and the liquidus are labelled with the melt fraction by weight. (b) The total thickness of melt present below a given depth plotted as a function of depth, calculated by integrating the volume of melt present in (a).

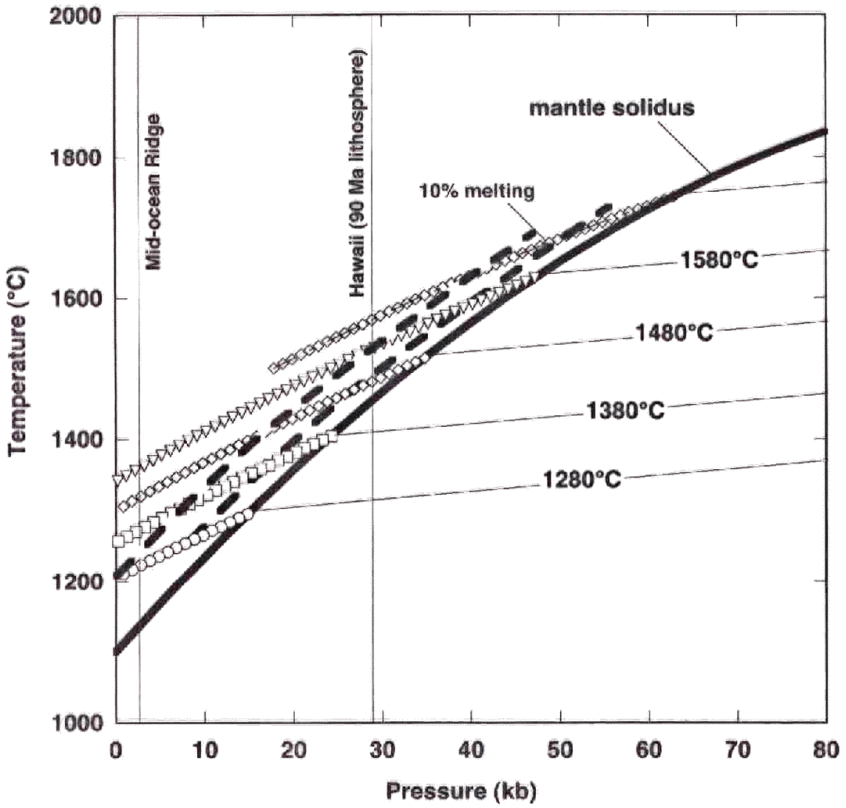

5. What happens "above the solidus" after melting starts?

- rate of melting is about 1% per kb
  or 0.3% per km

- melting requires 100 cal/g of melt produced (endothermic reaction)

- If you start with 100g of solid & melt it 1%, then you produce 1g of liquid and use up 100 cal of heat

- The heat required for melting is provided by cooling of the 99g of solid + 1g of liquid.

- The "specific heat" of the rock-liquid mixture is about 0.3 cal/g/°C (or 30 cal/100g/°C)

- Therefore, as 1% of melt is produced, the mantle cools by 3.3°C, which is in addition to the adiabatic cooling of 1°.

- So the slope $\frac{dT}{dP}$ above the solidus is ~4x greater than the adiabatic slope.

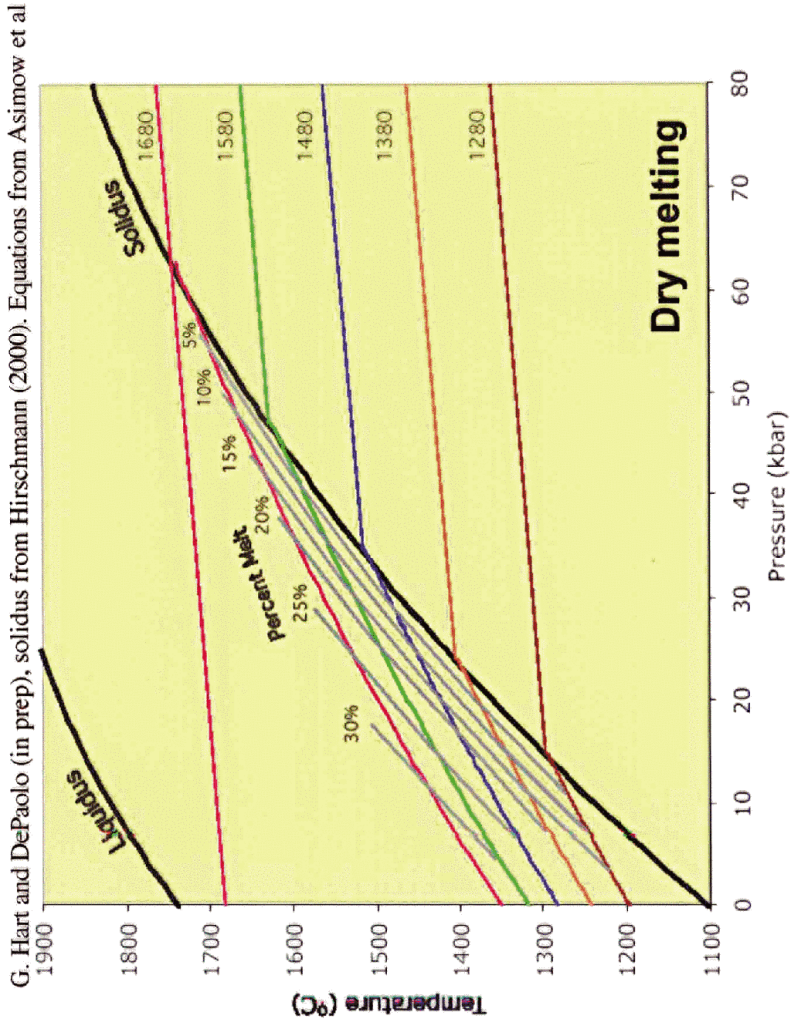
G. Hart and DePaolo (in prep), solidus from Hirschmann (2000). Equations from Asimow et al
Dry melting
Solidus
Liquidus
Percent Melt
5%
10%
15%
20%
25%
30%
1680
1580
1480
1380
1280
Temperature (°C)
Pressure (kbar)
1900
1800
1700
1600
1500
1400
1300
1200
1100
0
10
20
30
40
50
60
70
80

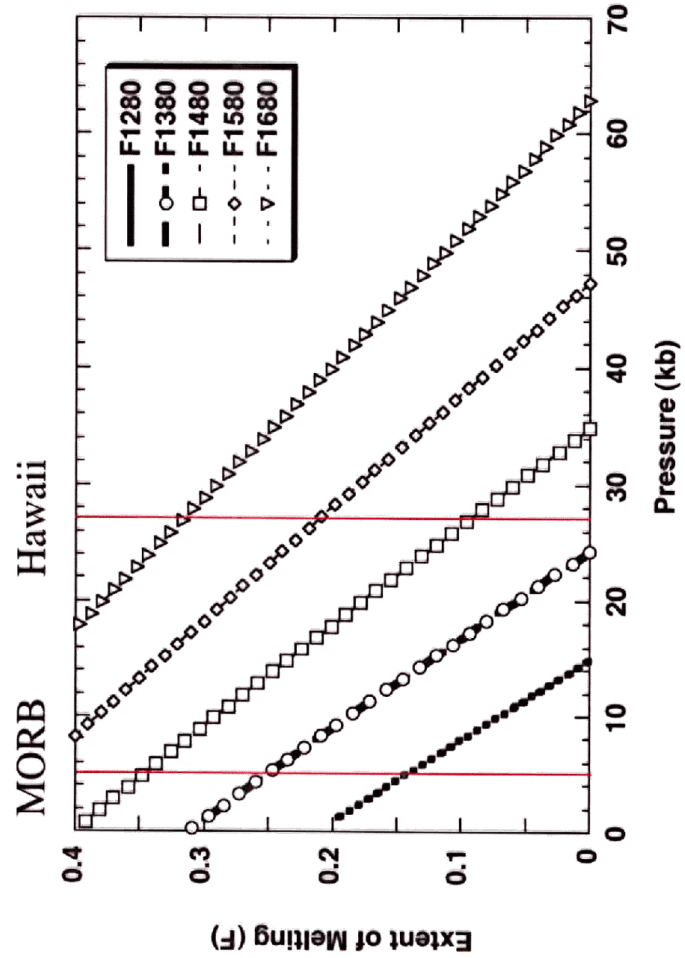
MORB
Hawaii
F1280
F1380
F1480
F1580
F1680
Extent of Melting (F)
Pressure (kb)
0.4
0.3
0.2
0.1
0
0
10
20
30
40
50
60
70

Magma generation rate

W = upwelling (upward) velocity of solid mantle rock (m/yr)

Γ = melting rate (fraction melted / meter of upward motion)

$\approx \frac{15\%}{40\,km} = .0035/km$

h = height of melting region (0 to ~120km)

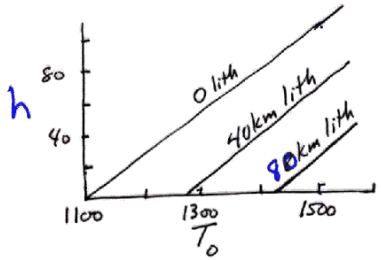

A = area of upwelling mantle rock

Total magma generation rate G

$$G = W\Gamma h A$$

For Hawaii

$W \approx 20\ cm/yr \approx 2\times10^{-4}\ km/yr$ (range is 0 - 100 cm/yr)

$h \approx 50\ km$

$A \approx 10^4\ km^2$

so $G \approx (2\times10^{-4})(.0035)(50)(10^4)$

$= 0.35\ km^3/yr$

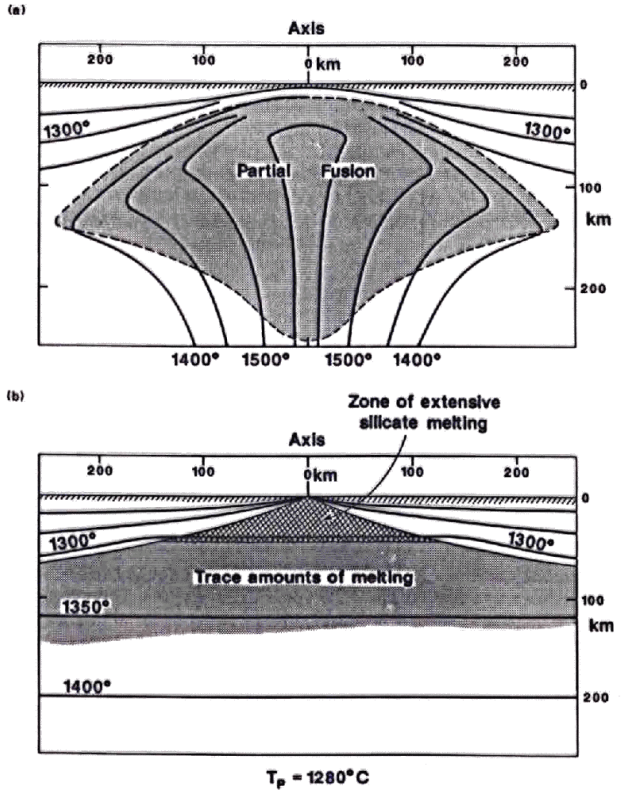

FIG. 2. (a) A sketch of the temperature distribution beneath a spreading ridge axis (from Oxburgh, 1980) when it coincides with a hot rising jet in the mantle. For reasons discussed in the text few spreading ridges are now believed to coincide with such jets, and must instead be passive features underlain by mantle of constant potential temperature. (b) Shows a sketch of the resulting temperature structure.

Making oceanic crust & the temperature of the mantle

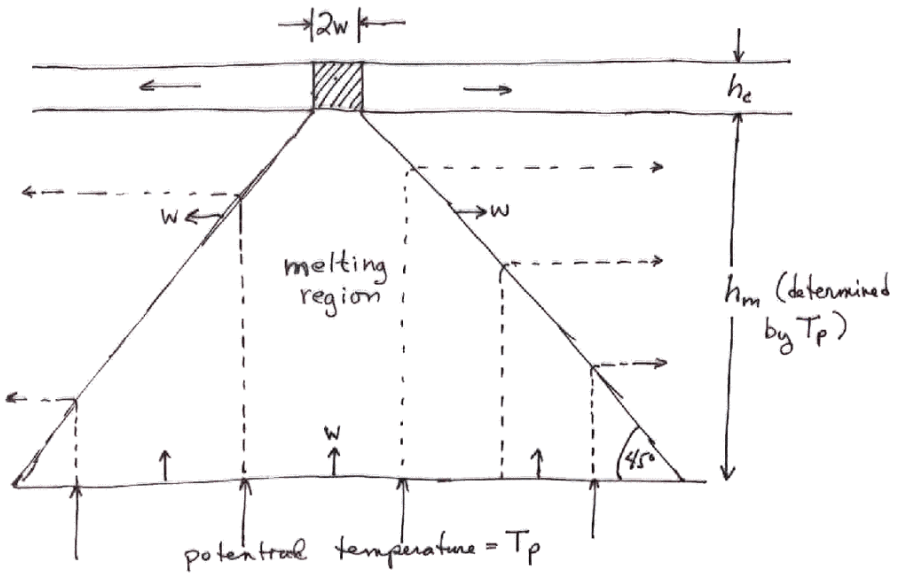

1. Area of melting region $\approx h_m^2$
2. For upward movement of the mantle by an amount = ω, spreading = 2ω occurs at the ridge
3. For "ω" in units of km, upward movement of ω km causes mantle to melt by about $0.35\% \cdot \omega$
4. Total amount of melt produced = $0.0035\, h_m^2 \omega = h_c \cdot 2\omega$

   so $h_c = \dfrac{0.0035\, h_m^2}{2}$
5. For $h_m = 40$ km, $h_c = 2.8$ km ($T_p \approx 1300°C$)

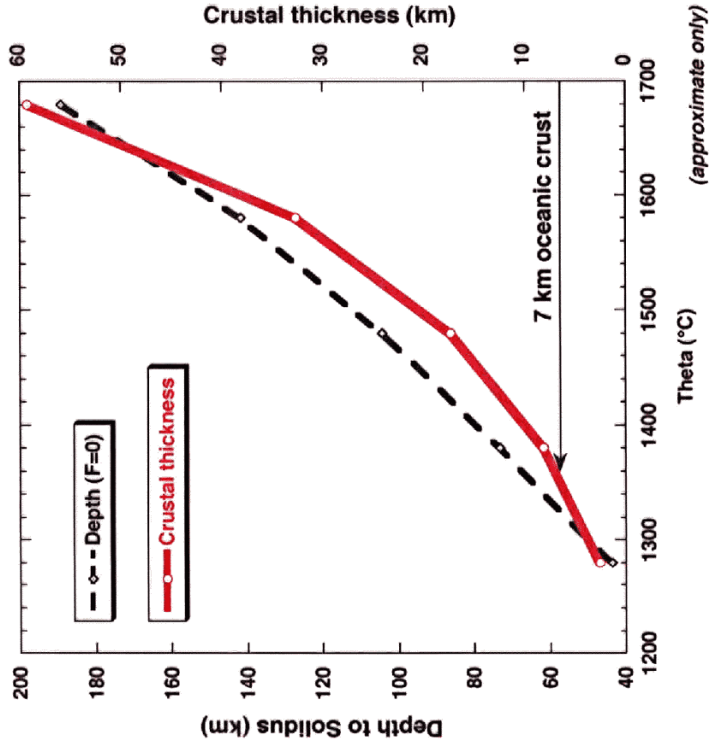

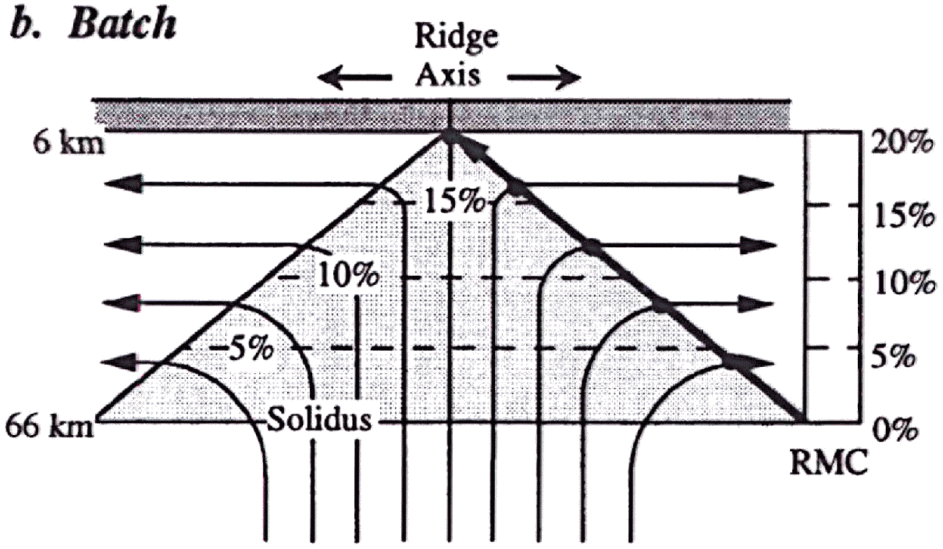

Spiegelman and McKenzie (1987)

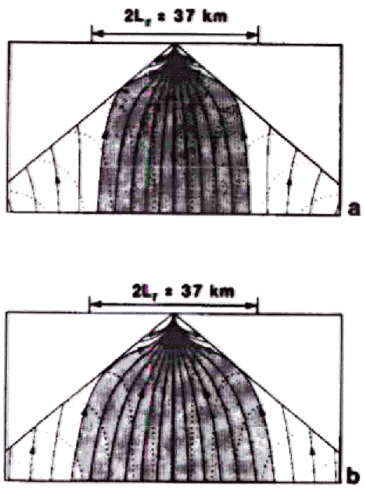

Fig. 2. Melt streamlines (solid) and matrix streamlines (dashed) for slow-spreading ridges, $U_0 = 1$ cm yr^{-1} ($\alpha = 40°$), matrix shear viscosity, $\eta = 10^{21}$ Pa s. Stippled region is the melt extraction zone containing all melt streamlines connecting the ridge axis to depth. h is the crustal thickness produced by the extraction zone. All figures are true scale. (a) Low porosity, $w_0/U_0 = 1.56$ ($\phi_0 = 1.0\%$), $h = 0.5$ km. (b) High porosity sufficient to produce ~ 6 km of crust, $w_0/U_0 = 9.12$ ($\phi_0 = 2.4\%$), $h = 6.5$ km.

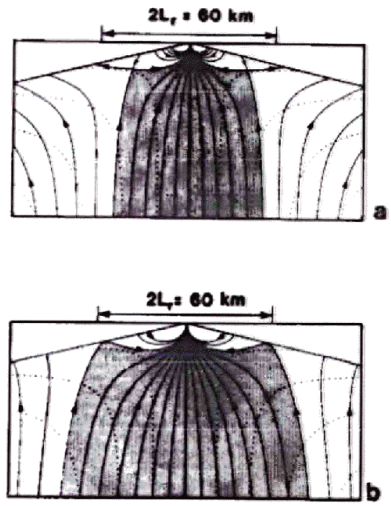

Fig. 3. Melt and matrix streamlines for fast spreading ridges. $U_0 = 7.5$ cm yr^{-1} ($\alpha = 13°$). $\eta = 10^{21}$ Pa s. (a) Low porosity, showing saddlepoint in the melt stream function, $w_0/U_0 = 0.47$ ($\phi_0 = 1.5\%$), $h = 0.5$ km. (b) High porosity, sufficient to produce ~ 6 km of crust, $w_0/U_0 = 2.77$ ($\phi_0 = 3.6\%$), $h = 6.1$ km.